

# Synthesis, structural characterization, and solid-state NMR spectroscopy of $[\text{Ga}(\text{phen})(\text{H}_{1.5}\text{PO}_4)_2] \cdot \text{H}_2\text{O}$ and $[\text{Ga}(\text{phen})(\text{HPO}_4)(\text{H}_2\text{PO}_4)] \cdot 1.5\text{H}_2\text{O}$ (*phen* = 1, 10-phenanthroline), two organic–inorganic hybrid compounds with 1-D chain structures

Wen-Jung Chang<sup>a</sup>, Pai-Ching Chang<sup>a</sup>, Hsien-Ming Kao<sup>a</sup>, Kwang-Hwa Lii<sup>a,b,\*</sup>

<sup>a</sup>Department of Chemistry, National Central University, Chungli, Taiwan 320, ROC

<sup>b</sup>Institute of Chemistry, Academia Sinica, Taipei, Taiwan 115, ROC

Received 6 August 2005; received in revised form 19 September 2005; accepted 20 September 2005  
Available online 25 October 2005

## Abstract

Two new organic–inorganic hybrid compounds,  $[\text{Ga}(\text{phen})(\text{H}_{1.5}\text{PO}_4)_2] \cdot \text{H}_2\text{O}$  (**1**) and  $[\text{Ga}(\text{phen})(\text{HPO}_4)(\text{H}_2\text{PO}_4)] \cdot 1.5\text{H}_2\text{O}$  (**2**) (*phen* = 1,10-phenanthroline), have been synthesized by hydrothermal methods and structurally characterized by single-crystal X-ray diffraction, infrared spectroscopy, thermogravimetric analysis, and solid-state NMR spectroscopy. Their structures consist of 1-D chains of strictly alternating  $\text{GaO}_4\text{N}_2$  octahedra and phosphate tetrahedra. The *phen* ligands in both compounds bind in a bidentate fashion to the gallium atoms and the 1-D structures extend into 3-D supramolecular arrays via  $\pi$ – $\pi$  stacking interactions of *phen* ligands and hydrogen bonds.  $^2\text{H}$  MAS NMR spectroscopy was applied to study the deuterated sample of **1** which contains very short hydrogen bonds with an  $\text{O} \cdots \text{O}$  distance of 2.406(2) Å. Crystal data for **1**: monoclinic, space group  $C2/c$  (No. 15),  $a = 11.077(1)$  Å,  $b = 21.496(2)$  Å,  $c = 7.9989(7)$  Å,  $\beta = 127.211(2)^\circ$ , and  $Z = 4$ . The crystal symmetry is the same for **2** as for **1** except  $a = 27.555(2)$  Å,  $b = 6.3501(5)$  Å,  $c = 21.327(2)$  Å,  $\beta = 122.498(1)^\circ$ , and  $Z = 8$ .

© 2005 Elsevier Inc. All rights reserved.

**Keywords:** Phosphate; Gallium; Phenanthroline; Crystal structure; Solid state NMR

## 1. Introduction

Recently, many research activities have focused on the synthesis of open-framework metal phosphates with organic ligands. The underlying idea is to combine the robustness of inorganic phosphate frameworks with the versatility and chemical flexibility of organic ligands. It has been established that oxalate readily substitutes for phosphate in the skeletons of inorganic phosphates forming a large number of oxalate–phosphate hybrid compounds [1]. Another class of organic–inorganic hybrid compounds is based on 4,4'-bipyridine and phosphate, in which the metal cations are coordinated by both types of

ligands [2]. In these structures, the 4,4'-bpy unit can act as a diprotonated counter cation, a monoprotated pendant ligand or as a neutral bridging ligand. About a half of the reported structures in this system consist of metal phosphate layers pillared by 4,4'-bpy ligands. This structure type exhibits the characteristic pattern of alternating organic–inorganic domains often observed in metal organophosphonate phases. Recently, we were interested in using 2,2'-bipyridine (bpy) or 1,10-phenanthroline (*phen*) to synthesize new organic–inorganic hybrid compounds, and have isolated the first fluorinated metal phosphates with bpy ligand, namely  $\text{Fe}_2\text{F}_2(2,2'\text{-bpy})(\text{HPO}_4)_2(\text{H}_2\text{O})$  and the gallium analogue [3]. A good number of metal phosphates with bpy and *phen* ligands have been reported [4]. Herein, we describe the synthesis and structural characterization of two new members in this family,  $[\text{Ga}(\text{phen})(\text{H}_{1.5}\text{PO}_4)_2] \cdot \text{H}_2\text{O}$  (denoted as **1**) and  $[\text{Ga}(\text{phen})(\text{HPO}_4)$

\*Corresponding author. Department of Chemistry, National Central University, Chungli, Taiwan 320, ROC. Fax: +886 3 422 7664.

E-mail address: [liikh@cc.ncu.edu.tw](mailto:liikh@cc.ncu.edu.tw) (K.-H. Lii).

(H<sub>2</sub>PO<sub>4</sub>)·1.5H<sub>2</sub>O (denoted as **2**), which are similar in composition, but adopt different structures. Compound **1** is particularly interesting in that its 1-D chain structure contains very short hydrogen bonds with an O⋯O distance of 2.406(2) Å. Because the resolution of <sup>1</sup>H MAS NMR spectra is often hindered by the huge <sup>1</sup>H–<sup>1</sup>H dipolar interactions and is also complicated by the background signals from the probe head, <sup>2</sup>H magic angle spinning (MAS) NMR spectroscopy was applied to study the deuterated sample of **1**.

## 2. Experimental section

### 2.1. Synthesis and initial characterization

The hydrothermal reactions were carried out in Teflon-lined stainless steel Parr acid digestion bombs under autogeneous pressure. A reaction mixture of Ga<sub>2</sub>O<sub>3</sub> (1 mmol), 1,10-phenanthroline (2 mmol), H<sub>3</sub>PO<sub>4</sub> (9 mmol), LiBO<sub>2</sub> (2 mmol), hydrofluoric acid (9 mmol) and H<sub>2</sub>O (10 mL) was heated at 190 °C for 3 days followed by slow cooling to room temperature at 10 °C/h. The solid product was filtered off, washed with water, rinsed with ethanol and dried at room temperature to give colorless columnar crystals of **1** in 83.9% yield based on Ga. Elemental analysis confirmed its stoichiometry. *Anal. Found*: C, 31.24; H, 2.71; N, 5.99%. *Calc.*: C, 31.24; H, 2.82; N, 6.07% for **1**. A deuterated sample was synthesized in a yield of 75.7% by reacting Ga<sub>2</sub>O<sub>3</sub> (1 mmol), 1,10-phenanthroline (2 mmol), H<sub>3</sub>PO<sub>4</sub> (9 mmol), LiBO<sub>2</sub> (2 mmol), hydrofluoric acid (9 mmol) and D<sub>2</sub>O (10 mL) under the same reaction conditions. We have carried out retro-syntheses without LiBO<sub>2</sub> in the reaction mixture; the resulting product is Ga<sub>2</sub>F<sub>2</sub>(1,10-phen)(HPO<sub>4</sub>)<sub>2</sub>(H<sub>2</sub>O), which is isostructural with Ga<sub>2</sub>F<sub>2</sub>(2,2'-bpy)(HPO<sub>4</sub>)<sub>2</sub>(H<sub>2</sub>O) [3]. We also noted that the addition of hydrofluoric acid helped growth of good quality crystals for structure analysis.

Colorless columnar crystals of compound **2** were obtained in a yield of 87.8% by heating Ga<sub>2</sub>O<sub>3</sub> (1 mmol), 1,10-phenanthroline (2 mmol), H<sub>3</sub>PO<sub>4</sub> (6 mmol), and H<sub>2</sub>O (10 mL) under the same reaction conditions as those for **1**. Elemental analysis confirmed its stoichiometry. *Anal. Found*: C, 30.30; H, 2.90; N, 5.70% *Calc.*: C, 30.67; H, 3.00; N, 5.96% for **2**.

Both products were monophasic because their X-ray powder patterns were in good agreement with the calculated patterns based on the atomic coordinates derived from single-crystal X-ray diffraction (Figures S1 and S2). Powder X-ray data were collected on a Shimadzu XRD-6000 powder diffractometer with CuK $\alpha$  radiation equipped with a scintillation detector. Data were collected in the range 5° < 2 $\theta$  < 50° using  $\theta$ –2 $\theta$  mode in a Bragg–Brentano geometry. The IR spectrum was recorded on a BIO-RAD FT-IR spectrometer within the range 400–4000 cm<sup>–1</sup> using the KBr pellet method. Thermogravimetric analysis was performed on a Perkin-Elmer TGA7 thermal analyzer; the sample was heated in flowing oxygen

from 40 to 600 °C at 10 °C/min and then the rate was changed to 5 °C/min from 600 to 900 °C.

### 2.2. Single-crystal X-ray diffraction

Colorless crystals of dimensions 0.03 × 0.05 × 0.07 and 0.03 × 0.05 × 0.15 mm for **1** and **2**, respectively, were selected for indexing and intensity data collection on Siemens Smart-CCD diffractometer equipped with a normal focus, 3-kW sealed tube X-ray source at room temperature. Empirical absorption corrections based on symmetry equivalents were performed by using the SADABS program for the Siemens area detector ( $T_{\text{min}/\text{mas}} = 0.894/0.979$  for **1**; 0.784/0.987 for **2**) [5]. The structures were solved by direct methods and refined by full-matrix least-squares on  $F^2$ . The gallium and phosphorus atoms were first located, and the carbon, nitrogen and oxygen atoms were found in subsequent difference Fourier maps. Bond-valence calculations indicate that O(2) and O(4) in **1** and O(4), O(6) and O(7) in **2** are hydroxo oxygen atoms, and O(5) in **1** and O(9) and O(10) in **2** are water oxygen atoms [6]. The hydrogen atoms bonded to oxygen atoms except O(10) in **2** were located in difference Fourier maps. The H(O2) atom in **1** sits on a 2-fold axis to form symmetrical H-bonds with O(2)–H(O2) bond length of 1.204 Å and O(2)–H(O2)–O(2) bond angle of 176.5°. The hydrogen atoms, which are bonded to carbon atoms, were positioned geometrically and refined using a rigid model with fixed isotropic thermal parameters. The final cycles of least-squares refinement included atomic coordinates and anisotropic thermal parameters for all non-hydrogen atoms. The atomic coordinates and isotropic thermal parameters for framework hydrogen atoms were fixed ( $U = 0.05 \text{ \AA}^2$ ). The reliability factors converged to  $R_1 = 0.0347$ ,  $wR_2 = 0.0827$ , and  $S = 0.928$  for **1** and  $R_1 = 0.0414$ ,  $wR_2 = 0.1034$ , and  $S = 0.913$  for **2**. All calculations were performed using SHELXTL Version 5.1 software package [7]. The crystallographic data are given in Table 1 and selected bond distances in Table 2. CIF file for **1** and **2** has been deposited with the Cambridge Crystallographic Data Centre as Supplementary publication no. CCDC-280320 & 280321.

### 2.3. Solid-state NMR measurements

<sup>2</sup>H MAS NMR experiments were performed at 76.75 MHz on a Varian Infinityplus-500 NMR spectrometer equipped with a 2.5 mm Chemagnetics probe. The 90° pulse length, the dwell time, and the recycle delay were 3.5, 2  $\mu$ s, and 1 s, respectively. The spinning speed was controlled at 20 kHz. The spectrum was referenced to CDCl<sub>3</sub> at 7.24 ppm as an external reference. The <sup>2</sup>H MAS NMR spectrum was simulated by the STARS software to obtain the <sup>2</sup>H quadrupolar coupling constant [8].

Table 1  
The crystallographic data for [Ga(phen)(H<sub>1.5</sub>PO<sub>4</sub>)<sub>2</sub>]·H<sub>2</sub>O (**1**) and [Ga(phen)(HPO<sub>4</sub>)(H<sub>2</sub>PO<sub>4</sub>)]·1.5H<sub>2</sub>O (**2**)

	1	2
Chemical formula	C <sub>12</sub> H <sub>13</sub> N <sub>2</sub> O <sub>9</sub> P <sub>2</sub> Ga	C <sub>12</sub> H <sub>14</sub> N <sub>2</sub> O <sub>9.5</sub> P <sub>2</sub> Ga
<i>a</i> /Å	11.077(1)	27.555(2)
<i>b</i> /Å	21.496(2)	6.3501(5)
<i>c</i> /Å	7.9989(7)	21.327(2)
β/deg	127.211(2)	122.498(1)
<i>V</i> /Å <sup>3</sup>	1516.8(2)	3147.4(4)
<i>Z</i>	4	8
Formula weight	460.90	469.91
Space group	C2/ <i>c</i> (No. 15)	C2/ <i>c</i> (No. 15)
<i>T</i> , K	296	296
λ(MoKα), Å	0.71073	0.71073
<i>D</i> <sub>calc</sub> , g/cm <sup>3</sup>	2.018	1.983
μ(MoKα), cm <sup>-1</sup>	20.8	20.1
<i>R</i> <sub>1</sub> <sup>a</sup>	0.0347	0.0414
w <i>R</i> <sub>2</sub> <sup>b</sup>	0.0827	0.1034

$$^a R_1 = \sum ||F_o| - |F_c|| / \sum |F_o|$$

$$^b wR_2 = [\sum w(F_o^2 - F_c^2)^2 / \sum w(F_o^2)]^{1/2}, \quad w = 1/[\sigma^2(F_o^2) + (aP)^2 + bP], \quad P = [\text{Max}(F_o^2, 0) + 2(F_c^2)]/3, \quad \text{where } a = 0.0323 \text{ and } b = 0 \text{ for } \mathbf{1} \text{ and } a = 0.0496 \text{ and } b = 0 \text{ for } \mathbf{2}.$$

Table 2  
Selected bond lengths (Å) for [Ga(phen)(H<sub>1.5</sub>PO<sub>4</sub>)<sub>2</sub>]·H<sub>2</sub>O (**1**) and [Ga(phen)(HPO<sub>4</sub>)(H<sub>2</sub>PO<sub>4</sub>)]·1.5H<sub>2</sub>O (**2**)<sup>a</sup>

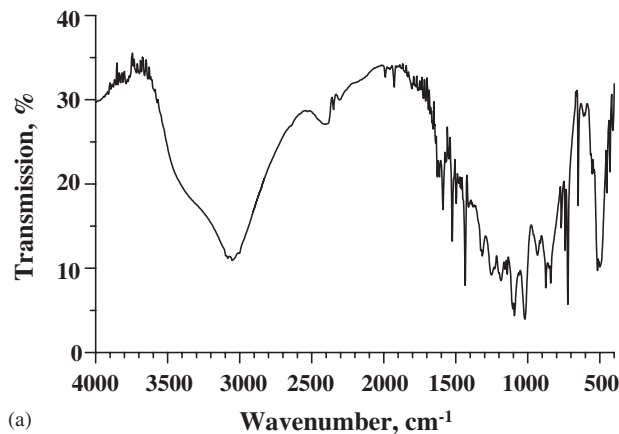
Compound 1			
Ga(1)–O(1)	1.998(2) (2 ×)	Ga(1)–O(3)	1.893(2) (2 ×)
Ga(1)–N(1)	2.091(2) (2 ×)	P(1)–O(1)	1.525(2)
P(1)–O(2)	1.514(2)	P(1)–O(3)	1.504(2)
P(1)–O(4)	1.576(2)	O(2)–H(O2)	1.204
O(4)–H(O4)	0.906	O(5)–H(O5)	0.890 (2 ×)
Compound 2			
Ga(1)–O(1)	1.960(2)	Ga(1)–O(2)	1.960(2)
Ga(1)–O(3)	1.882(2)	Ga(1)–O(5)	1.938(2)
Ga(1)–N(1)	2.131(3)	Ga(1)–N(2)	2.083(3)
P(1)–O(1)	1.522(2)	P(1)–O(2)	1.532(2)
P(1)–O(3)	1.503(2)	P(1)–O(4)	1.572(2)
P(2)–O(5)	1.507(2)	P(2)–O(6)	1.572(3)
P(2)–O(7)	1.556(3)	P(2)–O(8)	1.496(3)
O(4)–H(O4)	0.873	O(6)–H(O6)	1.078
O(7)–H(O7)	0.906	O(9)–H(O9A)	0.955
O(9)–H(O9B)	0.887		

<sup>a</sup>The C–H bond lengths are 0.93 Å.

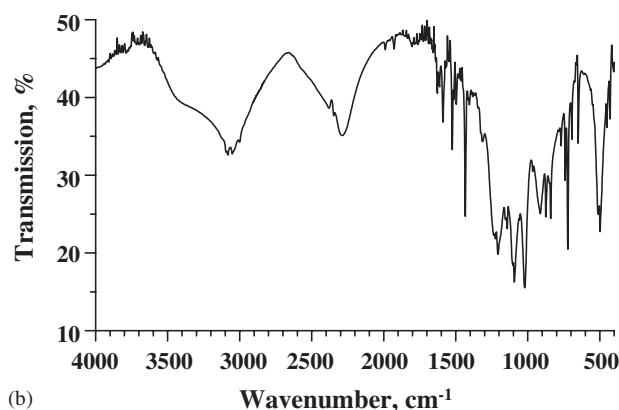
### 3. Results and discussion

#### 3.1. Infrared spectroscopy and thermogravimetric analysis

As shown in Fig. 1 the IR spectrum of **1** displays bands characteristic of hydrogen-bonded O–H stretch [ $\nu(\text{O–H})$ –3250 cm<sup>-1</sup>] and the stretching of C–H bonds on the *sp*<sup>2</sup> carbon hybrids and the stretching of C–C bonds in the phenanthroline ring [ $\nu(\text{C–H})$  = 3052 cm<sup>-1</sup>,  $\nu(\text{C–C})$  = 1588, 1524, 1435, 1316, 1186, 870, 841, 733, and 650 cm<sup>-1</sup>], thus confirming the organic component and a



(a)



(b)

Fig. 1. FTIR spectrum of **1** (a) and the deuterated sample (b).

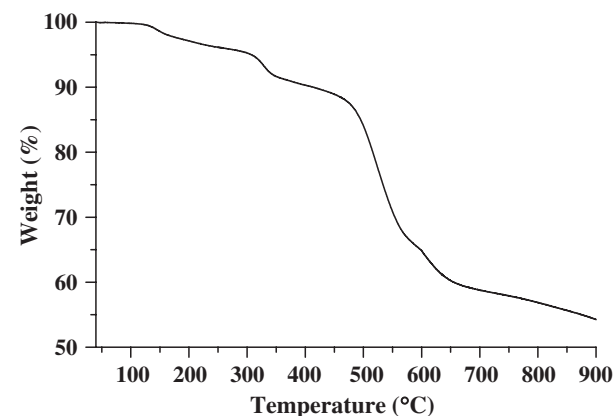


Fig. 2. The TG curve for **1** in flowing oxygen.

water molecule. The two peaks at 1020 and 1094 cm<sup>-1</sup> correspond to the stretching vibrations of P–O bonds. The deuterated sample shows a stretching vibration of O–D at 2288 cm<sup>-1</sup>, and the band near 3250 cm<sup>-1</sup> is reduced in intensity, indicating that only the OH and H<sub>2</sub>O hydrogens are partially replaced by deuterium.

The TG curve for **1** shows a broad weight loss in several overlapping steps, which commences gradually at ca. 125 °C and is incomplete by 900 °C (Fig. 2). The X-ray of powder pattern of the decomposition product shows a

broad peak centered at about  $2\theta = 24^\circ$ , which is indicative of an amorphous material. The first step between 125 and 300 °C corresponds to the loss of the lattice water molecules (obsd: 4.75%; calcd: 3.91%). A further weight loss of 41% occurs in several steps between 300 and 900 °C, which can be attributed to the removal of 1  $C_{12}H_8N_2$  and 1.5  $H_2O$  due to the dehydration of 2  $H_{1.5}PO_4$  groups (calcd: 44.96%). The total weight loss between 30 and 900 °C is ca. 45.75%, which is smaller than the calculated value of 48.87% probably because of incomplete decomposition.

### 3.2. Description of the structures

$[Ga(phen)(H_{1.5}PO_4)_2] \cdot H_2O$  (1): Compound **1** crystallizes in the monoclinic space group  $C2/c$  with a unit cell content of four formula units. Ga(1) and H(2O) have a local symmetry of  $C_2$  and all other atoms are at general positions. Fig. 3(a) shows the coordination environment of

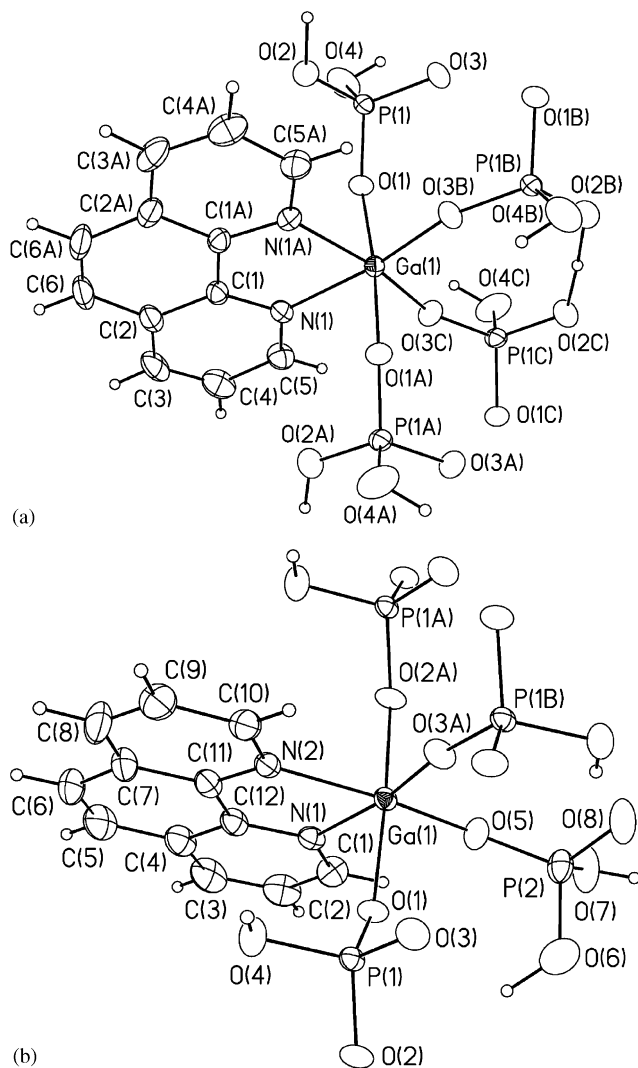


Fig. 3. The coordination environment of Ga atom in the structure of **1** (a) and **2** (b). Thermal ellipsoids are shown at 50% probability. Small open circles represent H atoms.

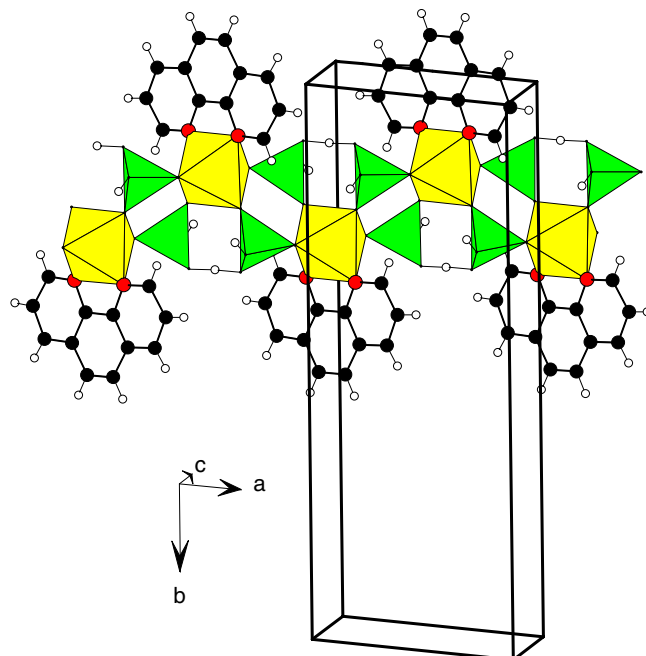


Fig. 4. Section of an infinite chain in **1**. The yellow and green polyhedra are gallium octahedra and phosphate tetrahedra, respectively. Key: black circles, C atoms; red circles, N atoms; small open circles, H atoms.

Ga(1). The Ga atom is octahedrally coordinated by one bidentate *phen* and four phosphate ligands. Compound **1** has a 1-D chain structure. The fundamental building units include a  $GaO_4N_2$  octahedron, a hydrogen phosphate tetrahedron, a *phen* ligand, and a lattice water molecule. The connectivity between units is made by phosphate group that joins neighboring two octahedra to form infinite chains parallel to the  $[101]$  direction (Fig. 4). Of the remaining two P(1)–O bonds, the longest one constitutes the P–O(4)H group which extends away from the chain, while the other (P–O(2)) is bonded to a hydrogen atom on a 2-fold axis, which is also shared by an adjacent phosphate group bonded to the same Ga atom. The O(2)–H bond length in the symmetrical O(2)–H–O(2) bonds is 1.204(2) Å. The hydrogen bond is extremely short and strong (O(2)⋯O(2) = 2.406 Å,  $\angle$  O(2)–H–O(2) = 176.5°). The very short O⋯O distance indicates that the H atom is likely at mid-point. However, we cannot exclude the possibility that the H atom is dynamically disordered over two positions related by a 2-fold axis. The location of the H atom has to be determined accurately by neutron diffraction. The infinite chains are held in position by hydrogen bonds between lattice water molecules and phosphate ligands (Fig. 5). In addition neighboring *phen* ligands from adjacent chains have a structure of parallel stacking and are separated by 4.00 Å, indicating significant attractive intermolecular aromatic interaction (Fig. 6). Thus, gallium phosphate chains are extended into a 3-D supramolecular array via H-bonds and  $\pi$ - $\pi$  stacking interactions.

$[Ga(phen)(HPO_4)(H_2PO_4)] \cdot 1.5H_2O$  (2): Compound **2** crystallizes in the monoclinic space group  $C2/c$  with a unit cell content of eight formula units. One of the lattice water

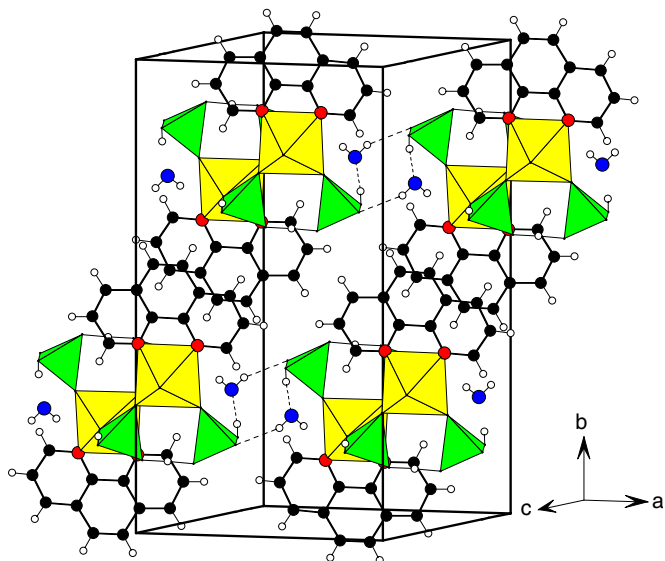


Fig. 5. Structure of **1** showing the hydrogen bonds between lattice water molecules and phosphate ligands and the  $\pi$ - $\pi$  stacking interactions between neighboring 1,10-*phen* ligands from adjacent chains. Key: blue circles, water oxygen atoms.

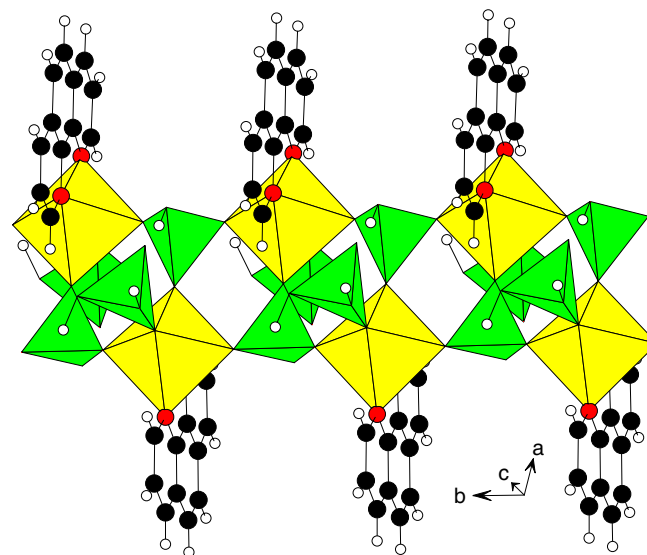


Fig. 7. Section of an infinite chain in **2**. The yellow and green polyhedra are gallium octahedra and phosphate tetrahedra, respectively. Key: black circles, C atoms; red circles, N atoms; small open circles, H atoms.

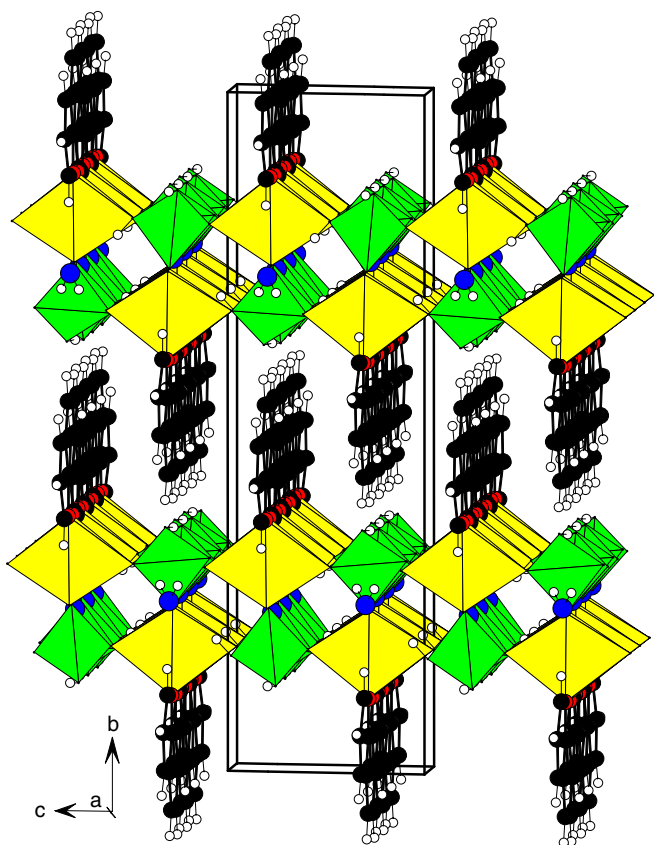


Fig. 6. Structure of **1** viewed in a direction approximately parallel to the *a* axis.

molecules, H<sub>2</sub>O(10), has a local symmetry of  $C_2$  and all other atoms are at general positions. Fig. 3(b) shows the coordination environment of Ga(1). The Ga atom is octahedrally coordinated by one bidentate *phen*, 1

H<sub>2</sub>PO<sub>4</sub>, and three HPO<sub>4</sub> ligands. Compound **2** also has a 1-D chain structure. The fundamental building units include 1 GaO<sub>4</sub>N<sub>2</sub> octahedron, 1 HPO<sub>4</sub>, 1 H<sub>2</sub>PO<sub>4</sub>, 1 *phen* ligand, and 2 lattice water molecules. The connectivity between units is made by HPO<sub>4</sub> that joins neighboring three octahedra to form infinite chains parallel to the [010] direction (Fig. 7). H<sub>2</sub>PO<sub>4</sub> has one oxygen bridging to GaO<sub>4</sub>N<sub>2</sub> and extends away from the chain as a pendant group, which accounts for the relatively larger thermal parameters of the atoms in the group. Of the remaining three P(2)–O bonds, the longer two constitute the P–OH groups, while the third is a terminal P–O bond possessing multiple bond character (P(2)–O(8) = 1.496 Å). The infinite chains are held in position by hydrogen bonds between the pendant H<sub>2</sub>PO<sub>4</sub> groups and attractive intermolecular aromatic interaction between *phen* ligands into a 3-D supramolecular array (Fig. 8). H<sub>2</sub>O(9) is strongly hydrogen-bonded to the pendant H<sub>2</sub>PO<sub>4</sub> group, whereas H<sub>2</sub>O(10) does not form any hydrogen bonds with the phosphate oxygen atoms, which explains the very large thermal parameters for O(10). Adjacent *phen* ligands are parallel and separated by 3.17 Å, which indicates strong  $\pi$ - $\pi$  interactions.

*Related structures:* Fig. 9 is a schematic representation of 1-D chains in **1** and **2**. Both chains consist of four-membered rings formed by two gallium octahedra and two phosphate tetrahedra via corner-sharing. In the structure of **2** there is a H<sub>2</sub>PO<sub>4</sub> attached to each metal atom as a pendant group. Several 1-D hybrid chain structures in the M/1,10-*phen* (or 2,2'-bpy)/phosphate systems have been reported. Compound **1** displays a new type of 1-D architecture, whereas the chain in **2** has also been observed in [Fe(*phen*)(HPO<sub>4</sub>)(H<sub>2</sub>PO<sub>4</sub>)]·0.5H<sub>2</sub>O and [Cd(*phen*)(H<sub>2</sub>PO<sub>4</sub>)<sub>2</sub>]·H<sub>2</sub>O [9,10]. The four-membered rings in the

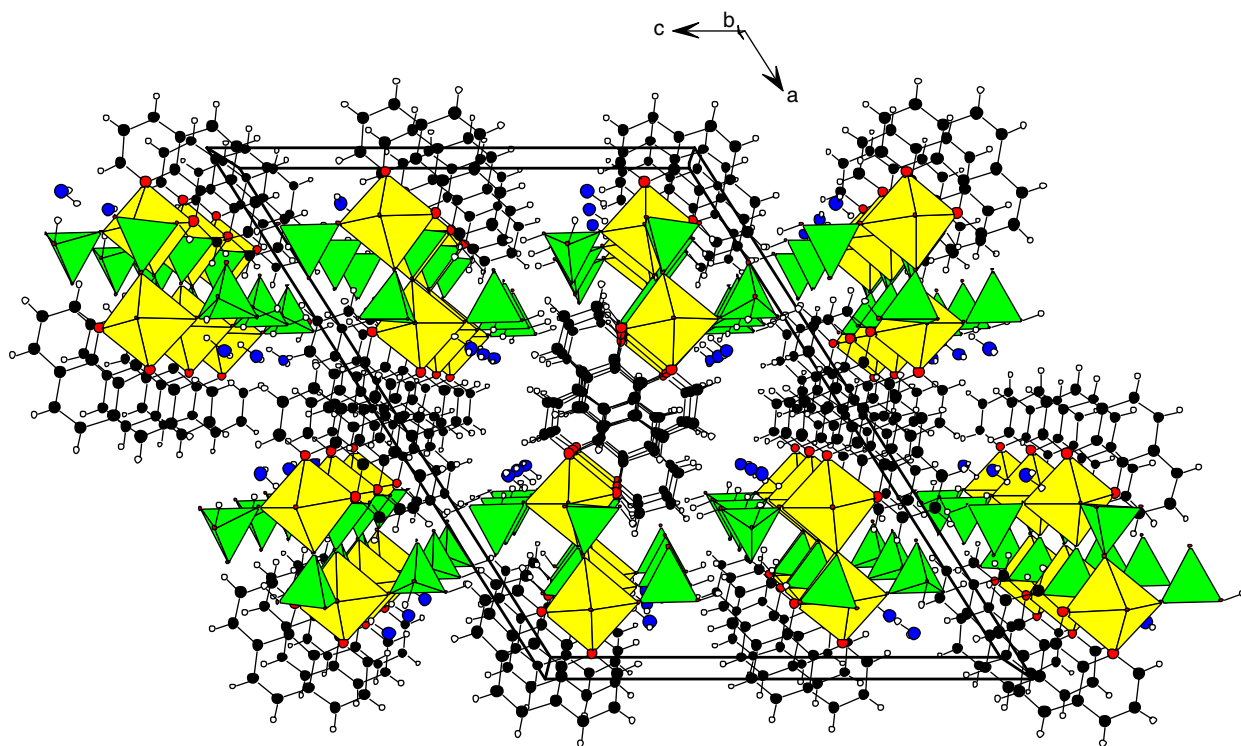


Fig. 8. Structure of **2** viewed along the *b*-axis. Key: blue circles, water oxygen atoms.

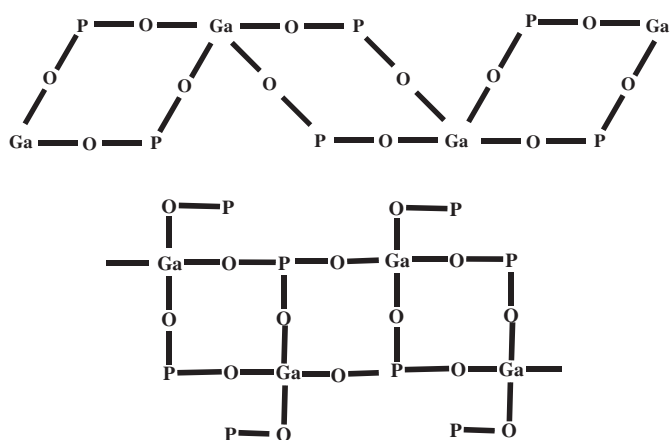


Fig. 9. Schematic representation of a chain in **1** (top) and **2** (bottom). The 1,10-*phen* ligands are not shown.

1-D chains of the anhydrous organic–inorganic hybrid,  $\text{Cd}(2,2'\text{-bpy})(\text{H}_2\text{PO}_4)_2$ , are linked by  $\text{Cd}-\text{O}-\text{Cd}$  bonds through 3-coordinated oxygen atoms [11]. In contrast to **2**, the anhydrous gallium phosphate,  $\text{Ga}(2,2'\text{-bpy})(\text{HPO}_4)(\text{H}_2\text{PO}_4)$ , adopts a 2-D layer structure [12].

**$^2\text{H}$  MAS NMR Spectroscopy:** The  $^2\text{H}$  MAS NMR spectrum of deuterated sample of **1** is shown in Fig. 10. Two isotropic peaks at 14.2 and 8.6 ppm, associated with a shoulder at 5.5 ppm, with large sideband manifolds were observed in the spectrum (inset of Fig. 10). The sideband manifolds associated with the isotropic peak at 14.2 ppm exhibit a characteristic symmetric line shape (Pake-doub-

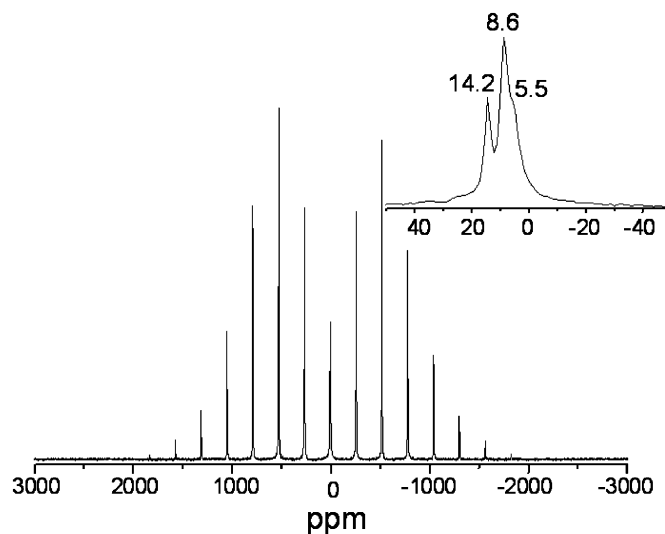


Fig. 10.  $^2\text{H}$  MAS NMR spectrum of **1** collected at r.t. at a spinning speed of 20 kHz. The isotropic resonances are labeled in the inset. All other peaks are spinning sidebands.

let) [13], indicating the deuterons are rigid in the time scale of the  $^2\text{H}$  MAS NMR experiments. Simulation of the spectrum yielded a QCC value of 190 ( $\pm 2$ ) kHz for this resonance, which is consistent with the typical QCC value of 160–240 kHz for an O–D environment in an inorganic solid [14]. Thus, the isotropic peak at 14.2 ppm is assigned to O(2)–D–O(2) hydrogen bond. The broader peak at 8.6 ppm and the shoulder at 5.5 ppm can be ascribed to PO(4)–D group and lattice water, respectively.

In summary, two new organic–inorganic hybrid compounds with similar compositions but different structures have been synthesized by hydrothermal reactions. The syntheses have many parameters and a subtle change in the reaction conditions can greatly affect the course of the reactions. It appears that the addition of  $\text{LiBO}_2$  to the reaction mixture is important to the formation of **1** and HF facilitates the crystal growth. Both compounds consist of 1-D chains of gallium phosphate which are extended into 3-D supramolecular arrays via hydrogen bonds and  $\pi$ – $\pi$  stacking interactions of *phen* ligands. The presence of very short hydrogen bond in **1** is verified by  $^2\text{H}$  MAS NMR spectroscopy. Compound **1** displays a new type of 1-D architecture, whereas the chain in **2** has been observed in the iron and cadmium analogues. The M/*phen* (or bpy)/ $\text{PO}_4$  phases have a rich structural chemistry. Further research on this interesting system is in progress.

### Acknowledgments

The authors thank Ms. F.-L. Liao and Professor S.-L. Wang at National Tsing Hua University for X-ray data collection and the National Science Council of Taiwan for financial support.

### Appendix A. Supplementary materials

Supplementary data associated with this article can be found in the online version at [doi:10.1016/j.jssc.2005.09.028](https://doi.org/10.1016/j.jssc.2005.09.028).

### References

- [1] (a) H.-M. Lin, K.-H. Lii, Y.-C. Jiang, S.-L. Wang, *Chem. Mater.* 11 (1999) 519;
- (b) L.-C. Huang, H.-M. Kao, K.-H. Lii, *Chem. Mater.* 12 (2000) 2441;
- (c) Y.-C. Jiang, S.-L. Wang, S.-F. Lee, K.-H. Lii, *Inorg. Chem.* 42 (2003) 6154;
- (d) Z.A.D. Lethbridge, P. Lightfoot, *J. Solid State Chem.* 143 (1999) 58;
- (e) Z.A.D. Lethbridge, S.K. Tiwary, A. Harrison, P. Lightfoot, *J. Chem. Soc. Dalton Trans.* (2001) 1904;
- (f) S. Natarajan, *J. Solid State Chem.* 139 (1998) 200;
- (g) A. Choudhury, S. Natarajan, C.N.R. Rao, *J. Solid State Chem.* 146 (1999) 538;
- (h) A. Choudhury, S. Natarajan, C.N.R. Rao, *Chem.-A Eur. J.* 6 (2000) 1168;
- (i) J. Do, R.P. Bontchev, A.J. Jacobson, *Chem. Mater.* 13 (2001) 2601;
- (j) C.T.S. Choi, E.V. Anokhina, C.S. Day, Y. Zhao, F. Taulelle, C. Huguenard, Z. Gan, A. Lachgar, *Chem. Mater.* 14 (2002) 4096.
- [2] (a) K.-H. Lii, Y.-F. Huang, *Inorg. Chem.* 38 (1999) 1348;
- (b) C.-Y. Chen, F.-R. Lo, H.-M. Kao, K.-H. Lii, *Chem. Commun.* (2000) 1061;
- (c) Y.-C. Jiang, Y.-C. Lai, S.-L. Wang, K.-H. Lii, *Inorg. Chem.* 40 (2001) 5320;
- (d) L.-H. Huang, H.-M. Kao, K.-H. Lii, *Inorg. Chem.* 41 (2002) 2936;
- (e) L.-I. Hung, S.-L. Wang, H.-M. Kao, K.-H. Lii, *Inorg. Chem.* 41 (2002) 3929;
- (f) W.-K. Chang, R.-K. Chiang, Y.-C. Jiang, S.-L. Wang, S.-F. Lee, K.-H. Lii, *Inorg. Chem.* 43 (2004) 2564;
- (g) Z. Shi, S. Feng, S. Gao, L. Zhang, G. Yang, J. Hua, *Angew. Chem. Int. Ed.* 39 (2000) 2325.
- [3] W.-J. Chang, C.-Y. Chen, K.-H. Lii, *J. Solid State Chem.* 172 (2003) 6.
- [4] (a) Y. Zhang, R.C. Haushalter, J. Zubieta, *Inorg. Chim. Acta* 260 (1997) 105;
- (b) R. Finn, J. Zubieta, *Chem. Commun.* (2000) 1321;
- (c) Z. Shi, S. Feng, L. Zhang, G. Yang, J. Hua, *Chem. Mater.* 12 (2000) 2930;
- (d) W. Yang, C. Lu, *Inorg. Chem.* 41 (2002) 5638;
- (e) Y. Lu, E. Wang, M. Yuan, G. Luan, Y. Li, H. Zhang, C. Hu, Y. Yao, Y. Qin, Y. Chen, *J. Chem. Soc. Dalton Trans.* (2002) 3029;
- (f) Z.-E. Lin, Y.-Q. Sun, J. Zhang, Q.-H. Wei, G.-Y. Yang, *J. Mater. Chem.* 13 (2003) 447;
- (g) Z.-E. Lin, J. Zhang, S.-T. Zheng, G.-Y. Yang, *Inorg. Chem. Commun.* 6 (2003) 1035;
- (h) Z.-E. Lin, J. Zhang, Y.-Q. Sun, G.-Y. Yang, *Inorg. Chem.* 43 (2004) 797.
- [5] G.M. Sheldrick, SADABS, Program for Siemens Area Detector Absorption Corrections, University of Göttingen, Germany, 1997.
- [6] I.D. Brown, D. Altermatt, *Acta Crystallogr. B* 41 (1985) 244.
- [7] G.M. Sheldrick, SHELXTL Programs, Version 5.1, Bruker AXS GmbH, Karlsruhe, Germany, 1998.
- [8] J. Skibsted, N.C. Nielsen, H. Bildsøe, H.J. Jakobsen, *J. Magn. Reson.* 95 (1991) 88.
- [9] H. Meng, G. Li, Y. Liu, L. Liu, Y. Cui, W. Pang, *J. Solid State Chem.* 177 (2004) 4459.
- [10] Z.-E. Lin, J. Zhang, S.-T. Zheng, G.-Y. Yang, *Solid State Sci.* 7 (2005) 319.
- [11] Z.-E. Lin, Y.-Q. Sun, J. Zhang, Q.-H. Wei, G.-Y. Yang, *J. Mater. Chem.* 13 (2003) 447.
- [12] Z.-E. Lin, J. Zhang, Y.-Q. Sun, G.-Y. Yang, *Inorg. Chem.* 43 (2004) 797.
- [13] G.E. Pake, *J. Chem. Phys.* 16 (1948) 327.
- [14] (a) R.J. Wittebort, M.G. Usha, D.J. Ruben, D.E. Wemmer, A. Pines, *J. Am. Chem. Soc.* 110 (1988) 5668;
- (b) T. Lin, J.A. DiNatale, R.R. Vold, *J. Am. Chem. Soc.* 116 (1994) 2133;
- (c) H. Lee, T. Polenova, R.H. Beer, A.E. McDermott, *J. Am. Chem. Soc.* 121 (1999) 6884.